Title

Measurement of the N*- - N*++ Mass Difference

Authors

Gidal, George
Kernan, Anne
Kim, Sedong

Publication Date

1965-08-01

UCRL-16096 Rev.

University of California

Ernest O. Lawrence Radiation Laboratory

MEASUREMENT OF THE $N^{*-} - N^{*++}$ MASS DIFFERENCE

Berkeley, California

DISCLAIMER

UNIVERSITY OF CALIFORNIA

Lawrence Radiation Laboratory
Berkeley, California

AEC Contract No. W-7405-eng-48

Sept. 23, 1965

ERRATUM

TO: All recipients of UCRL-16096 Rev.

FROM: Technical Information Division

Subject: UCRL-16096 Rev., MEASUREMENT OF THE $N^{*-} - N^{*++}$ MASS DIFFERENCE, George Gidal, Anne Kernan, and Sedong Kim. August 17, 1965

Please make the following correction on subject report:

Page 11, second equation reads: " $\sigma(\omega) \propto \dfrac{\omega_0^2 \Gamma^2(\omega)}{(\omega_0 - \omega)^2 + \omega_0^2 \Gamma^2(\omega)}$ "

It should read: " $\sigma(\omega) \propto \dfrac{\omega_0^2 \Gamma^2(\omega)}{(\omega_0^2 - \omega^2)^2 + \omega_0^2 \Gamma^2(\omega)}$ "

Submitted to Physical Review

UCRL-16096 Rev.

UNIVERSITY OF CALIFORNIA

Lawrence Radiation Laboratory
Berkeley, California

AEC Contract No. W-7405-eng-48

MEASUREMENT OF THE $N^{*-} - N^{*++}$ MASS DIFFERENCE

George Gidal, Anne Kernan, and Sedong Kim

August 17, 1965

Measurement of the $N^{*-} - N^{*++}$ Mass Difference*

George Gidal,† Anne Kernan, and Sedong Kim

Lawrence Radiation Laboratory
University of California
Berkeley, California

August 17, 1965

ABSTRACT

A measurement of the mass and width difference of N^{*-}-N^{*++} is described, where N^* is the nucleon resonance with $I(J^P) = 3/2(3/2^+)$ and mass approximately 1240 MeV. The resonances were produced in the inelastic reactions $n\,n \rightarrow p\,n\,\pi^-$ and $p\,p \rightarrow n\,p\,\pi^+$, which are known to proceed almost entirely via N^{*-} and N^{*++} production, respectively, in the observed energy region. A comparison of the $(n\,\pi^-)$ and $(p\,\pi^+)$ effective mass distributions gives a mass difference of 7.9 ± 6.8 MeV and a width difference of 25 ± 23 MeV for $N^{*-} - N^{*++}$. This result agrees with predictions based on the SU(3) and SU(6) symmetry schemes.

We report here a measurement of the N^{*-}-N^{*++} mass difference[1] $\delta\omega_0$ and width difference $\delta\Gamma_0$, N^* is the nucleon resonance of isotopic spin 3/2, $J^P = 3/2^+$, and mass approximately 1240 MeV.

The resonances were produced in the inelastic reactions

$$n\,n \rightarrow p_1\,n_2\,\pi_3^-, \tag{1}$$

$$p\,p \rightarrow n_1\,p_2\,\pi_3^+, \tag{2}$$

at a mean c.m. energy of 2.35 BeV. At this energy Reactions (1) and (2) are known to proceed almost entirely via N^{*-} and N^{*++} production respectively.[2,3] We determined $\delta\omega_0$ and $\delta\Gamma_0$ by a comparison of the distributions in the invariant mass, ω_{23}, for both reactions.

In the SU(3) symmetry scheme N^* is a member of the $J^P = 3/2^+$ decuplet, along with Y^*, Ξ^*, and Ω^-. Okubo[4] has recently pointed out that, because of electromagnetic mass splitting, the Gell-Mann-Okubo[5] mass formula is valid only for particles with the same charge, and in particular a knowledge of the N^{*-} mass is required for the comparison $\Omega^- - \Xi^{*-} = \Xi^{*-} - Y^{*-} = Y^{*-} - N^{*-}$. The decay width of N^{*-} is also needed to test the predicted relationship between the decay amplitudes of the decuplet particles Ξ^*, Y^*, and N^*.[6] In addition, the measured mass difference can be compared with the predictions of the various symmetry schemes.

In Section I of the paper the predictions of electromagnetic mass splittings within the framework of the SU(3) and SU(6) symmetry schemes are discussed. Section II contains the experimental details, and Section III considers possible systematic errors in the data. Section IV presents the results, and discusses the problem of elucidating resonance parameters from plots of invariant mass. In Section V the experimental measurement is compared with predictions based on the SU(3) and SU(6) symmetry schemes.

I. Electromagnetic Mass Splitting

The masses of particles within a given SU(2) representation are believed to be identical in the limit of isotopic spin invariance. The electromagnetic force removes this degeneracy, giving rise to mass differences of the order of αm_π (α is the fine-structure constant). In principle, the mass differences within an isomultiplet are obtainable by a calculation of the electromagnetic self-energies of the particles therein. The attempts to calculate self-energies for strongly interacting particles, within the framework of a perturbative expansion of field theory, have been unsuccessful.

In the unitary symmetry scheme isomultiplets of different hypercharge are grouped into "supermultiplets" (or unitary multiplets) which are the irreducible representations of the SU(3) group. It is postulated that, in the limit of exact unitary symmetry, the masses of all particles within a given SU(3) representation are identical. The observed mass differences between isomultiplets within a unitary multiplet are of the order of 100 MeV, and are believed to arise from the "medium-strong" force. By making the assumption that unitary symmetry is violated only by the electromagnetic interaction, it is possible to relate the mass splittings within different isomultiplets of a supermultiplet. In the baryon octet, for example, the prediction[7] of $\Xi^- - \Xi^0 = \Sigma^- - \Sigma^+ + p - n$ has been experimentally confirmed.[8] For the $3/2^+$ decuplet, of which N^* is a member, the relationship

$$m = m_0 + aQ + bQ^2 \qquad (3)$$

is predicted,[9] where Q is the charge and a and b are constants.

Coleman and Glashow have noted that the mass splittings within an SU(3) supermultiplet follow an octet pattern, and have proposed a dynamical theory of unitary symmetry violation, namely that symmetry-breaking

processes are dominated by "tadpole" diagrams because of the existence of an octet of scalar mesons.[10] For the $3/2^+$ decuplet such an octet dominance leads to an "equal-spacing" rule for electromagnetic splitting,

$$N^{*++} - N^{*+} = N^{*+} - N^{*0} = N^{*0} - N^{*-},$$
$$= Y^{*+} - Y^{*0} = Y^{*0} - Y^{*-} = \Xi^{*0} - \Xi^{*-}.$$

It also gives an intramultiplet relationship

$$\frac{N^{*++} - N^{*+}}{N^* - Y^*} = \frac{\Sigma^+ - \Sigma^-}{N - \Xi},$$

which yields $N^{*++} - N^{*+} = -3.0$ MeV and $N^{*++} - N^{*-} = -9.1$ MeV. These predictions must, however, be modified by the contributions of other mass-splitting diagrams. The leading nontadpole contribution to the electromagnetic self-masses of baryons comes from intermediate states containing one baryon and one photon.[11] The tadpole and nontadpole contributions to the electromagnetic mass differences are shown in Table I.

Dashen and Frautschi have proposed a bootstrap mechanism to explain octet dominance of the mass splitting.[12] Higher-order effects in this model again reduce the splitting and alter the equal-spacing pattern.

The group SU(6) contains both SU(2) and SU(3) as subgroups. In the recently proposed SU(6) symmetry scheme the baryon octet and the $J^P = 3/2^+$ decuplet are assigned to the 56-dimensional representation of SU(6).[13] The relations between the 10 mass differences in the 56-dimensional representation have been derived in the limit where SU(6) symmetry is broken by electromagnetism only:[14]

$$\begin{aligned}
\Xi^- - \Xi^0 &= (\Sigma^- - \Sigma^+) - (n - p), \\
N^{*0} - N^{*+} &= Y^{*0} - Y^{*+} = n - p, \\
N^{*-} - N^{*0} &= Y^{*-} - Y^{*0} = \Xi^{*-} - \Xi^{*0} \\
&= (n - p) + (\Sigma^- + \Sigma^+ - 2\Sigma^0), \\
N^{*-} - N^{*++} &= 3(n - p). \qquad (4)
\end{aligned}$$

The relationships between the decuplet members are identical with Eq. (3).

II. Experimental Details

Two conditions are desirable to achieve a precise measurement:

(a) Reactions (1) and (2) should occur under identical experimental conditions.

(b) Both reactions should occur at the same energy.

Condition (b) is necessary because the shape of the invariant-mass plot depends on the production mechanism, and no quantitative description of the production mechanism as a function of energy is available. By observing N^* production in charge-symmetric reactions at the same energy one ensures that any difference in the invariant-mass plots is due to electromagnetic effects only.

The reactions were simultaneously achieved at the same energy and under identical experimental conditions by the interactions of a beam of 3.64-BeV/c separated deuterons[15] with deuterium in the Brookhaven National Laboratory 20-inch bubble chamber. In the majority of d-d collisions one nucleon in each deuteron is a spectator. Reactions (1) and (2) occurred in the interactions

$$d\,d \rightarrow p_s^T\, p_s^B\, p_1\, n_2\, \pi_3^- \qquad (1a)$$

and

$$d\,d \rightarrow n_s^T\, n_s^B\, n_1\, p_2\, \pi_3^+ \qquad (2a)$$

respectively; the subscript "s" denotes a spectator, either in the beam deuteron "B" or the target deuteron "T."

Selection of Events

In Reaction (1a) the target spectator proton is not seen in the bubble chamber in 70% of the interactions because its momentum is less than 90 MeV/c.

Therefore, we scanned for events with three outgoing charged particles, since the proton in the target deuteron is then clearly a spectator. All told, 2870 events were measured and constrained to the hypothesis:

$$d\,n \rightarrow p\,p\,n\,\pi^-, \qquad (1b)$$

assuming that the target neutron was at rest in the laboratory system. In addition to Reaction (1a), the (1b) events include the pn reactions: $d\,d \rightarrow n_s^B\, p_s^T\, p\, p\, \pi^-$. The subtraction of pn events from the sample is described below.

Reaction (2a) was found by scanning for events with two emergent positively charged particles, of which one is a π^+ meson. In Reaction (1a) the maximum π^--meson momentum is 900 MeV/c and its mean value is 350 MeV/c, and the π^+ meson in (2a) is thus readily identified by momentum and bubble density. All together, 1687 events were measured, and were constrained to Reaction (2) with a beam proton momentum of 1.82 ± 0.09 BeV/c and the target proton at rest. The momentum spread of the beam proton was obtained by transforming to the laboratory system the known proton momentum distribution in the beam deuteron rest system. The calculated distribution is approximated fairly closely by a Gaussian with $\sigma = 0.09$ BeV/c.

The effect of ignoring the target motion in constraining Reactions (1b) and (2) is to broaden the χ^2 distribution, relative to a χ^2 distribution for a genuine one-degree-of-freedom event. In a one-constraint fit the χ^2 value is approximately $[(MM - MN) / \Delta MM]^2$, where MM is the calculated missing mass, MN is the true mass of the outgoing neutral particle, and ΔMM is the experimental error in missing mass.

Neglect of the target momentum P_T shifts the missing mass downward by an amount $(T_T \cdot T_n - \underset{\sim}{P}_T \cdot \underset{\sim}{P}_n)/MM$, where T_T is the kinetic energy of the target particle and P_n and T_n are the momentum and kinetic energy of the

outgoing neutral particle. There is a correlation between large χ^2 values and high momenta of the outgoing neutral particle. For this reason it was necessary to accept all nn and pp events with $\chi^2 \leq 10$.

The χ^2 criterion was used to identify the events only; we did not use the constrained values of the particle momenta because of the uncertainty in the target momentum. In calculating the $(\pi^+ p)$ and $(\pi^- n)$ invariant masses we used the measured values of the particle momenta, and the neutron momentum was inferred from momentum conservation in Reaction (1b) with the target neutron assumed to be at rest. The neutron momentum is then uncertain by $\underset{\sim}{P}_T$, the target momentum, in addition to the usual measurement errors. In consequence, the calculated, $(\pi^- n)$ invariant mass, $\omega_{\pi^- n}$, is reduced from its true value by $\Delta Q = [(E_\pi/E_n) \cdot (\underset{\sim}{P}_n \cdot \underset{\sim}{P}_T) - (\underset{\sim}{P}_\pi \cdot \underset{\sim}{P}_T)]/\omega_{\pi^- n}$. A Monte Carlo calculation shows that ΔQ has a distribution with mean of -0.2 MeV, and root-mean-square deviation 6 MeV; its effect on the mass and width of the $(\pi^- n)$ distribution can therefore be ignored.

Two additional criteria were applied to enforce a correspondence between the nn and pp events.

(a) There may be a scanning bias against pp events with a short proton track. So we eliminated pp events with $P_p < 150$ MeV/c, and nn events with $P_n < 150$ MeV/c.

(b) The uncertainty in ω_{23} due to measurement errors is greater for $(\pi^- n)$ than for $(\pi^+ p)$. The average experimental error in ω_{23} is 30 MeV for $(\pi^- n)$ and 20 MeV for $(\pi^+ p)$. We eliminated all events with an error exceeding 20 MeV. (No correlation was observed between ω_{23} and its error.) Then the experimental error is the same in both reactions, and is small compared with the resonance width ($\Gamma_0 = 120$ MeV for N^{*++}). This condition is important because the value of the resonant mass inferred from the invariant-mass distribution is not independent of the width of the distribution.[16] A total of

1091 and 722 events satisfied the selection criteria for nn and pp interactions respectively.

Subtraction of np events in the Reaction $dn \rightarrow ppn\pi^-$

For the nn events in Reaction (1b) the beam proton is a spectator; in the pn event the beam neutron is a spectator. A beam spectator is identified by having a momentum of less than 120 MeV/c in the rest system of the beam deuteron. The transverse momentum distribution of such nucleons is shown in Fig. 1; it follows closely the Hulthén form of the deuteron wave function, giving evidence for the validity of the impulse approximation. In a total of 1091 dn interactions, 133 had a beam spectator neutron and did not have a beam spectator proton. (In a strongly peripheral interaction, the interacting nucleon is sometimes indistinguishable from a spectator.) The (π^-n) effective-mass distribution for these 133 events is shown in Fig. 2. They are clearly $pn \rightarrow pp\pi^-$ reactions, as there is no evidence of N^{*-} production. According to the measured nucleon-nucleon cross sections in this energy region the ratio of nn to pn interactions is 5.2.[17] The expected number of pn events is then 176; the discrepancy is due to the experimental error in the neutron momentum which can shift it outside the limits for a high-energy spectator—$1.4 < P < 2.3$ BeV, $0 \text{ deg} < \theta < 5 \text{ deg}$—where P is the neutron momentum and θ is the angle it makes with the beam. The histogram in Fig. 2 was normalized to a total of 176 events and subtracted from the (π^-n) invariant mass distribution (1091 events), to give the distribution in Fig. 3a. Figure 3b shows the (π^+p) invariant-mass plot in the pp reactions.

III. Possible Sources of Error

Since the N^{*-} mass is determined with a missing neutron whereas the N^{*++} is determined with two charged particles, systematic errors in the beam momentum or the magnetic field (or both) can simulate a mass difference. This

danger is avoided by using the value of the beam momentum obtained by curvature measurement on beam tracks in the bubble chamber. If the magnetic field value is incorrect (say, by 1%), the pion and proton momentum are overestimated by 1%, but the neutron momentum is similarly affected, since it is calculated as $\underset{\sim}{P}_n = \underset{\sim}{P}_d - \Sigma \underset{\sim}{P}_{\text{charged}}$. So, there is no spurious mass difference induced by an incorrect value for the magnetic field, provided the beam momentum is estimated by use of the same value for the magnetic field.

A systematic sagitta in the chamber would change the beam momentum and shift the $(\pi^- n)$ invariant-mass distribution. The maximum systematic curvature in the chamber has been estimated at 0.1×10^{-4} cm^{-1}, equivalent to 1% of the beam momentum.[18] A 1% change in beam momentum causes an average shift of 1 MeV in the effective mass. In fact, there is strong evidence that the systematic curvature in the chamber is considerably less than the maximum value quoted.[18]

In Reaction (1) target neutrons with momenta greater than 90 MeV/c are excluded. Hence the range of c.m. energies in Reaction (1) is restricted compared with Reaction (2). However, the requirement of a fit of Reaction (2) has the effect of excluding high Fermi momenta. As a check on the equality of the range of interaction energies for the two reactions, the pion and nucleon momentum distributions are compared in Figs. 4a, 4b. The coincidence of the momentum spectra leads us to believe that there is no bias here.

IV. Determination of the Resonance Parameters

The differential cross section for Reaction (1) is

$$d\sigma \propto |A|^2 \, \delta^4(P_f - P_i) \, \frac{d^3p_1 \, d^3p_2 \, d^3p_3}{E_1 E_2 E_3},$$

where A is the reaction amplitude. If A is known, one can calculate the

$(\pi^- n)$ invariant-mass distribution $\frac{d\sigma}{d\omega}(\omega, \omega_0, \Gamma_0)$. The most probable values of ω_0 and Γ_0 are those which minimize χ^2 when the experimental distribution in ω is fitted with $\frac{d\sigma}{d\omega}$. Because the production mechanism is not completely understood, no absolute determination of ω_0 and Γ_0 is attempted in this experiment.

Since the two resonances are produced in charge-symmetric reactions, we assume that the mass difference can be evaluated by use of an approximate expression for the amplitude. The validity of the approximation is tested by comparing the calculated N^{*++} parameters with the values measured directly in $\pi^+ p$ elastic scattering.

Analyses of Reactions (1) and (2) in this energy region[2,3] strongly indicate that: (a) the reactions go predominantly by one-pion exchange (OPE), and (b) the virtual π-nucleon scattering is dominated by the N^* resonant amplitude. We use these results to obtain an approximate expression for $\frac{d\sigma}{d\omega}$.

There are four OPE diagrams for Reaction (1) (Fig 5). The amplitude for the reaction is

$$A = A_a - A_b - A_c + A_d,$$

where the subscripts refer to the corresponding diagrams in Fig. 5. The interference terms $A_a A_d^*$ and $A_b A_c^*$ vanish because of the pseudoscalar nature of the pion, and it has been shown that the terms $A_a A_c^*$ and $A_b A_d^*$ are negligible.[19,20] Then

$$|A|^2 = |A_a|^2 + |A_b|^2 - 2 \operatorname{Re} A_a A_b^* + |A_c|^2 + |A_d|^2 - 2 \operatorname{Re} A_c A_d^*.$$

It is convenient to split $d\sigma$ into the sum of six terms, corresponding to these six terms:

$$d\sigma = d\sigma_a + d\sigma_b + d\sigma_{ab} + d\sigma_c + d\sigma_d + d\sigma_{cd}.$$

In the pole approximation (exchanged pion on the mass shell) the partial cross section $\frac{d\sigma_a}{d\omega}$ is[21]

$$\frac{d\sigma_a}{d\omega} \propto \int_{\Delta^2_{MIN}}^{\Delta^2_{MAX}} k\,\omega^2\,\sigma(\omega)\,\frac{\Delta^2}{(\Delta^2 + m_\pi^2)^2}\,d\Delta^2 = \sigma(\omega)\,f(\omega), \quad (5)$$

where ω is the $(\pi^- n)$ effective mass, k is the π^- momentum in the $(\pi^- n)$ rest frame, Δ^2 is the square of the four-momentum of the exchanged pion, and $\sigma(\omega)$ is the cross section at the four-particle vertex. It is clear that $\frac{d\sigma_a}{d\omega} = \frac{d\sigma_b}{d\omega}$ and $\frac{d\sigma_c}{d\omega} = \frac{d\sigma_d}{d\omega}$. We evaluated $\frac{d\sigma_{ab}}{d\omega}$, using the expression for $d\sigma_{ab}$ derived by Selleri in the pole approximation.[20] We found that $\frac{d\sigma_{ab}}{d\omega} = \sigma(\omega)\,f_I(\omega) \approx (0.6)\sigma(\omega)f(\omega)$. Since $f_I(\omega)$ is almost identical in form with $f(\omega)$, we made the approximation

$$\frac{d\sigma}{d\omega} \propto \frac{d\sigma_a}{d\omega} + \frac{d\sigma_c}{d\omega}.$$

Simple isotopic spin considerations show that, in the case of N^* dominance, charged-pion exchange predominates over neutral-pion exchange in the proportions 9:1. Therefore 90% of the events in Fig. 3a correspond to N^{*-} production $(d\sigma_a)$ and 10% to N^{*0} production $(d\sigma_c)$. The shape of the $(\pi^- n)$ effective-mass distribution for the $n\,n \rightarrow N^{*0}\,n$ events was approximated by the $(\pi^- p)$ effective mass distribution in Reaction (1) (Fig. 6). This distribution was normalized to 10% of the area in Fig. 3a and subtracted from it. The resulting distribution, shown in Fig. 7, corresponds to pure N^{*-} production and is described by $\frac{d\sigma_a}{d\omega}$. A similar procedure was used to eliminate the reflection of N^{*+} in the $(\pi^+ p)$ invariant-mass plot, giving the distribution in Fig. 7. The distributions in Fig. 7 contain a total of 695 nn and 558 pp events in the interval 1140 to 1320 MeV. These numbers do not reflect the

relative cross sections, because not all photographs used for the nn interactions were scanned for pp interactions.

The distributions in Fig. 7 were fitted with Eq. (5), modified by the off-mass-shell correction term[16]

$$\left[\frac{(\omega + m_2)^2 + \Delta^2}{(\omega + m_2)^2 - m_\pi^2}\right]^2 \left[\frac{(\omega - m_2)^2 + \Delta^2}{(\omega - m_2)^2 - m_\pi^2}\right].$$

The upper limit for Δ^2 was set at 0.8 $(\text{BeV}/c)^2$, according to the observed Δ^2 distribution in the nn reactions. In fact, the result is insensitive to a 50% variation in Δ^2_{MAX}. We use a single resonant p-wave amplitude for the π-nucleon cross section σ:

$$\sigma(\omega) \propto \frac{\omega_0^2 \Gamma^2(\omega)}{(\omega_0 - \omega)^2 + \omega_0^2 \Gamma^2(\omega)},$$

with $$\Gamma = \Gamma_0 (q/q_0)^3 \rho(\omega)/\rho(\omega_0),$$

where $\rho(\omega) = (a m_\pi^2 + q^2)^{-1}$ and $a = 1.3$ for m_π and q in MeV units;[16] q is the momentum of the decay products in the N^* rest frame. The values of ω_0 and Γ_0 which minimize χ^2 are shown in Table II. (It is reassuring that the N^{*++} parameters are in good agreement with the values measured in elastic $\pi^+ p$ scattering,[22,23] which are $\omega_0^{++} = 1236 \pm 0.5$ MeV, $\Gamma_0^{++} = 120 \pm 1.6$ MeV.)

In the absence of detailed knowledge of the reaction amplitude it is conventional to assume that the resonance and accompanying particles are produced according to phase space. This procedure is usually adequate for a narrow resonance ($\Gamma_0 < 50$ MeV). In Table II we give the resonance parameters obtained by fitting the distributions with the product of the three-body phase space and $\phi(\omega)$,[16] where $\phi(\omega) = C \frac{\omega}{q} \frac{\omega_0 \Gamma(\omega)}{(\omega_0^2 - \omega^2)^2 + \omega_0^2 \Gamma^2(\omega)}$; C is a normalization constant.

When, as for N^*, the width Γ is energy-dependent, the peak position in the invariant-mass plot, ω_{peak}, falls below ω_0, the shift $\omega_0 - \omega_{peak}$ being proportional to Γ_0^2. In order to locate the actual position of the peaks in the invariant-mass plots, we fitted them with an S-wave Breit-Wigner amplitude multiplied into phase space. This gives $\delta\omega_{peak} = 2.3 \pm 4.7$ MeV and $\delta\Gamma = 18 \pm 17$ MeV. Since the width of the ω^- distribution exceeds that of ω^{++}, one expects that $\delta\omega_0$ will be greater than $\delta\omega_{peak}$ when a P-wave Breit-Wigner form is used, and this is indeed the case.

The values obtained by the OPE fit, $\delta\omega_0 = 7.9 \pm 6.8$ MeV and $\delta\Gamma_0 = 25 \pm 23$ MeV, are taken as the best estimates of the resonance parameters. The error matrix for the masses and widths in the OPE fit is given in Table III, and for the mass and width difference in Table IV. There is a strong correlation between the estimated mass and width difference--the correlation coefficient is 0.73.

V. Discussion

Within the $3/2^+$ decuplet, the following additional mass differences have been reported:

$N^{*++} - N^{*0} = -0.45 \pm 0.85$ MeV (reference(23),),

$Y^{*-} - Y^{*+} = 17 \pm 7$ MeV (reference(24),),

$Y^{*-} - Y^{*+} = 4.3 \pm 2.2$ MeV (reference(25),),

$\Xi^{*-} - \Xi^{*0} = 5.7 \pm 3.0$ MeV (reference(26),),

$\Xi^{*-} - \Xi^{*0} = 7.0 \pm 4.7$ MeV (reference(27).).

These values, together with the value reported here, are compatible with Relations (3) and (4), with pure octet dominance, and with the modified tadpole theory. In particular, the SU(6) scheme predicts $\delta\omega_0 = N^{*-} - N^{*++} = 3.9$ MeV; pure octet dominance predicts $\delta\omega_0 = 9.0$ MeV; modified tadpole theory predicts

$\delta\omega_0 = 4.9$ MeV. It is clear that our errors prevent us from distinguishing among theories with predictions in this range. The value predicted for $\delta\omega_0$ by using the measurements of references 23 through 27 to evaluate the coefficients in Eq. (3) is $\delta\omega_0 = 5.0 \pm 1.5$.

Acknowledgments

We wish to thank the many members of the staff of the Brookhaven National Laboratory whose help made the experiment possible. In particular, we express our appreciation to Dr. Hildred Blewett, Dr. Hugh Brown, Dr. Ralph Shutt, and the AGS operating crew. We are indebted to Dr. Robert Birge, Dr. Jonas Shultz, Dr. Robert Socolow, and Dr. Frank Solmitz for helpful discussions, and to Dr. Robert Ely and Dr. George Kalmus for their work during the bubble chamber run. Finally, we thank the scanning and measuring staff of the Powell-Birge group and the Data Processing group under Mr. Howard White.

Table I. Tadpole and nontadpole contribution to the electromagnetic mass differences.

Mass difference	$A^{(a)}$	$B^{(b)}$	$C^{(c)}$
$N^{*++} - N^{*+}$	-3.0	0.2	4.4
$N^{*++} - N^{*0}$	-6.1	-2.9	2.7
$N^{*++} - N^{*-}$	-9.1	-9.1	-4.9
$Y^{*+} - Y^{*0}$	-3.0	-2.8	-1.4
$Y^{*+} - Y^{*-}$	-6.1	-9.1	-9.1
$Y^{*0} - Y^{*-}$	-3.0	-6.2	-7.6
$\Xi^{*0} - \Xi^{*-}$	-3.0	-6.3	-7.7

(a) A is the tadpole term alone.

(b) B is the tadpole term plus the self-energy diagrams with a baryon octet member and a photon in the intermediate state. (See Ref. 11, page 95.)

(c) C comprises B plus an estimate of the contribution to the self-energy diagrams from the decuplet channel. (See Ref. 11, page 102.)

Table II. Masses, widths, and mass differences for N^* (all in MeV).

		With P-wave Breit-Wigner amplitude		With S-Wave Breit-Wigner amplitude
		OPE	Phase space	Phase space
Mass ω_0	N^{*-}	1241.3 ± 5.1	1240.7 ± 6.1	1219.7 ± 3.4
	N^{*++}	1233.4 ± 4.4	1232.0 ± 4.9	1217.4 ± 3.2
Reduced width Γ_0	N^{*-}	149 ± 18	166 ± 21	133 ± 13
	N^{*++}	124 ± 14	137 ± 17	115 ± 11
Mass difference $\delta\omega_0$		7.9 ± 6.8	8.7 ± 7.8	2.3 ± 4.7
Width difference $\delta\Gamma_0$		25 ± 23	29 ± 27	18 ± 17

Table III. Error Matrix for masses and widths in the OPE fit [all in $(MeV)^2$].

	ω_0^-	Γ_0^-	ω_0^{++}	Γ_0^{++}
ω_0^-	26.2	69.6	.0	.0
Γ_0^-	69.6	326.	.0	.0
ω_0^{++}	.0	.0	19.7	43.9
Γ_0^{++}	.0	.0	43.9	201.

Table IV. Error Matrix for mass and width differences in the OPE fit [all in $(MeV)^2$].

	$\delta\omega_0$	$\delta\Gamma_0$
$\delta\omega_0$	45.9	113.
$\delta\Gamma_0$	113.	527.

Footnotes and References

* Work performed under auspices of U. S. Atomic Energy Commission.

† Presently on research leave at Istituto di Fisics dell'Universitá, Torino Italy.

1. A preliminary result of this experiment was presented at the 1964 International Conference on High Energy Physics, Dubna, U. S. S. R.
2. R. Birge, R. Ely, G. Gidal, G. Kalmus, A. Kernan, and S. Kim, The Reaction $n + n \rightarrow n + p + \pi^-$ at 1.9 GeV/c, Lawrence Radiation Laboratory Report UCRL-11550, July 1964 (unpublished).
3. D. V. Bugg, A. J. Oxley, J. A. Zoll, J. G. Rushbrooke, V. E. Barnes, J. B. Kinson, W. P. Dodd, G. A. Doran, and L. Riddiford, Phys. Rev. 133, B1017 (1964).
4. S. Okubo, J. Phys. Soc. Japan 19, 1507 (1964).
5. M. Gell-Mann, Phys. Rev. 125, 1067 (1962); S. Okubo, Progr. Theoret. Phys. (Kyoto) 27, 949 (1962).
6. C. Becchi, E. Eberle, and G. Morpurgo, Phys. Rev. 136, B808 (1964).
7. S. Coleman and S. L. Glashow, Phys. Rev. Letters 6, 423 (1961).
8. D. Carmony, G. Pjerrou, P. Schlein, W. Slater, D. Stork, and H. Ticho, Phys. Rev. Letters 12, 482 (1964), and other recent data cited therein; L. Jauneau, D. Morellet, U. Nguyen-Khac, et al., Phys. Letters 4, 49 (1963).
9. S. P. Rosen, Phys. Rev. Letters 11, 100 (1963); A. J. MacFarlane and E. C. G. Sudarshan, Nuovo Cimento 31, 1176 (1964).
10. S. Coleman and S. L. Glashow, Phys. Rev. 134, B671 (1964).
11. R. Socolow, Electromagnetic Masses in the Unitary Symmetry Theory (Ph. D. Thesis), Harvard University, May 1964 (unpublished).
12. R. Dashen and S. Frautschi, Phys. Rev. Letters 13, 497 (1964) and Phys. Rev. 137, B1331 (1965).

13. F. Gürsey and L. A. Radicati, Phys. Rev. Letters 13, 173 (1964); A. Pais, Phys. Rev. Letters 13, 175 (1964); B. Sakita, Phys. Rev. 136, B1756 (1964).

14. T. K. Kuo and Tsu Yao, Phys. Rev. Letters 14, 79 (1965).

15. C. Baltay, J. Sandweiss, J. Sanford, H. Brown, M. Webster, and S. Yamamoto, The Separated Beam at the AGS--Performance with Anti-protons and π^+ Mesons, in Proceedings of the 1962 Conference on Instrumentation for High Energy Physics, CERN, 1962 (North Holland Publishing Co., Amsterdam, Holland, 1962); J. Leitner, G. Moneti, and N. P. Samios, Performance of the AGS Separated Beam with High Energy Kaons, op. cit.

16. J. D. Jackson, Nuovo Cimento 34, 1644 (1964).

17. A. P. Batson, B. B. Culwick, H. B. Klepp, and L. Riddiford, Proc. Roy. Soc. (London) A, 251, 233 (1959).

18. R. I. Louttit, in Proceedings of the 1960 Conference on Instrumentation for High Energy Physics (Lawrence Radiation Laboratory, Berkeley, California), p. 117.

19. G. Da Prato, Nuovo Cimento 22, 123 (1961).

20. E. Ferrari and F. Selleri, Suppl. Nuovo Cimento 24, 453 (1962).

21. G. F. Chew and F. E. Low, Phys. Rev. 113, 1640 (1959).

22. N. Klepikov, V. Meshcheryakov, and S. Sokolov, Joint Institute for Nuclear Research (Dubna) Report JINR-D-584, 1960.

23. M. G. Olsson, Phys. Rev. Letters 14, 118 (1965).

24. W. A. Cooper, H. Filthuth, A. Fridman, E. Malamud, E. S. Gelsema, J. C. Kluyver, and A. G. Tenner, Phys. Letters 8, 365 (1964).

25. Darrell O. Huwe, Study of the Reaction $K^- p \rightarrow \Lambda \pi^+ \pi^-$ from 1.2 to 1.7 BeV/c (Ph. D. Thesis), Lawrence Radiation Laboratory Report UCRL-11291, July 1964 (unpublished).

26. G. M. Pjerrou, P. E. Schlein, W. E. Slater, L. T. Smith, D. H. Stork, and H. K. Ticho, Phys. Rev. Letters 14, 275 (1965).

27. G. W. London, Intrinsic and Dynamic Properties of the Ξ Hyperon, Dissertation Abstracts, 1964, p. 3060, (unpublished).

Figure Captions

Fig. 1. Distribution in transverse momentum, P_{TRAN}, of spectator nucleons in the beam deuterons. The smooth curve is the Fourier transform of the Hulthén wave function, folded into the transverse plane.

Fig. 2. The $(\pi^- n)$ invariant-mass distribution in the reaction $d\,n \rightarrow n_S^B\, p\, p\, \pi^-$, where n_S^B is a spectator neutron in the beam deuteron.

Fig. 3. (a) Distribution of the $(\pi^- n)$ invariant mass in the reaction $n\,n \rightarrow p\,n\,\pi^-$.

(b) Distribution of the $(\pi^+ p)$ invariant mass in the reaction $p\,p \rightarrow n\,p\,\pi^+$.

Fig. 4. (a) Normalized momentum distributions for π^- and π^+ in the reactions $n\,n \rightarrow n\,p\,\pi^-$ and $p\,p \rightarrow n\,p\,\pi^+$, respectively.

(b) Normalized momentum distributions for neutrons and protons in the reactions $n\,n \rightarrow n\,p\,\pi^-$ and $p\,p \rightarrow n\,p\,\pi^+$, respectively.

Fig. 5. Feynman diagrams for single-pion exchange in the reaction $n\,n \rightarrow p\,n\,\pi^-$.

Fig. 6. The $(\pi^- p)$ invariant-mass distribution in the reaction $n\,n \rightarrow p\,n\,\pi^-$.

Fig. 7. Invariant-mass distributions of $(\pi^- n)$ and $(\pi^+ p)$ in the reactions $n\,n \rightarrow n\,p\,\pi^-$ and $p\,p \rightarrow n\,p\,\pi^+$. The $(\pi^+ p)$ distribution (558 events) has been normalized to the area of the $(\pi^- n)$ distribution (695 events).

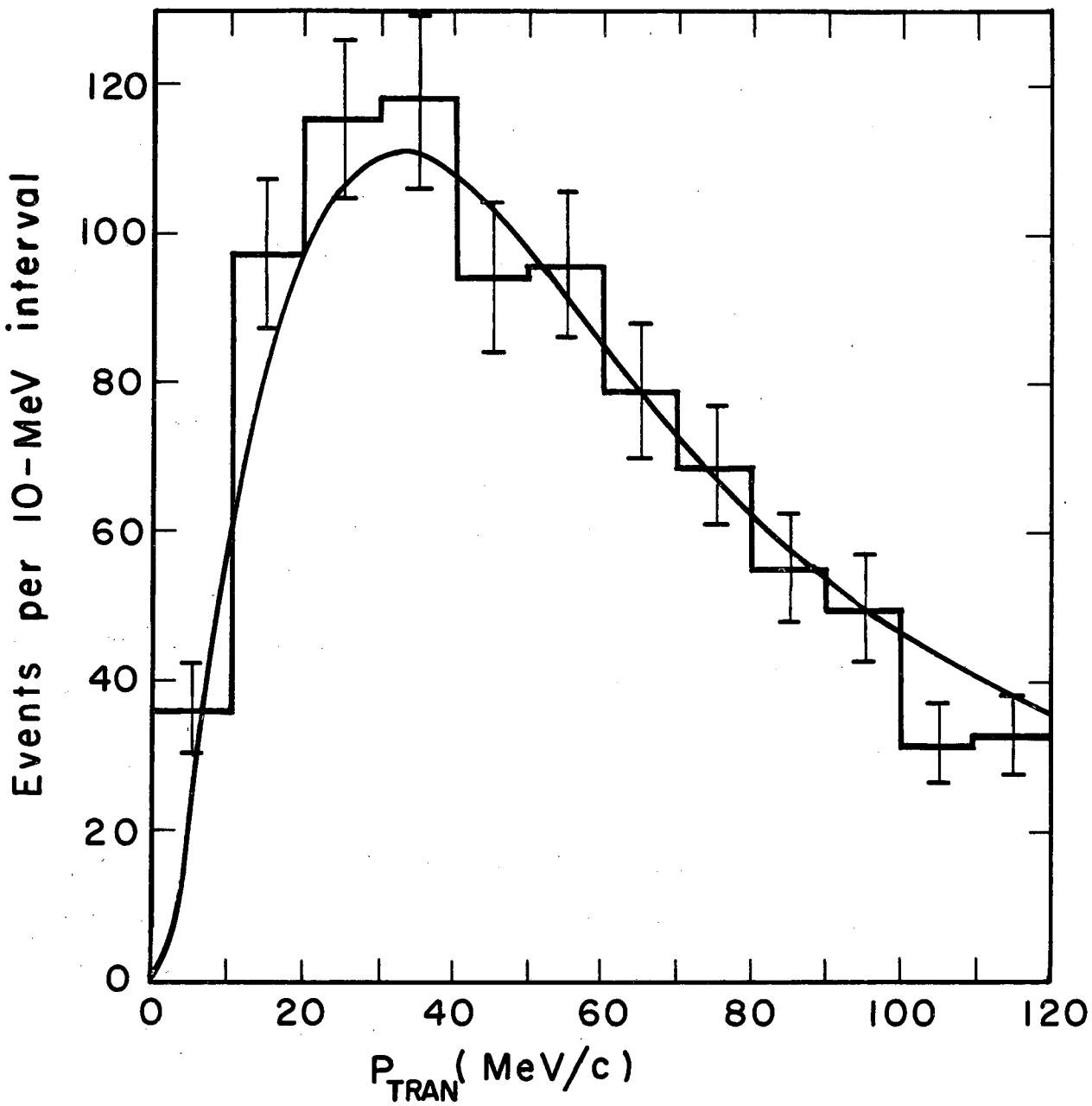

MUB-3352

Fig. 1

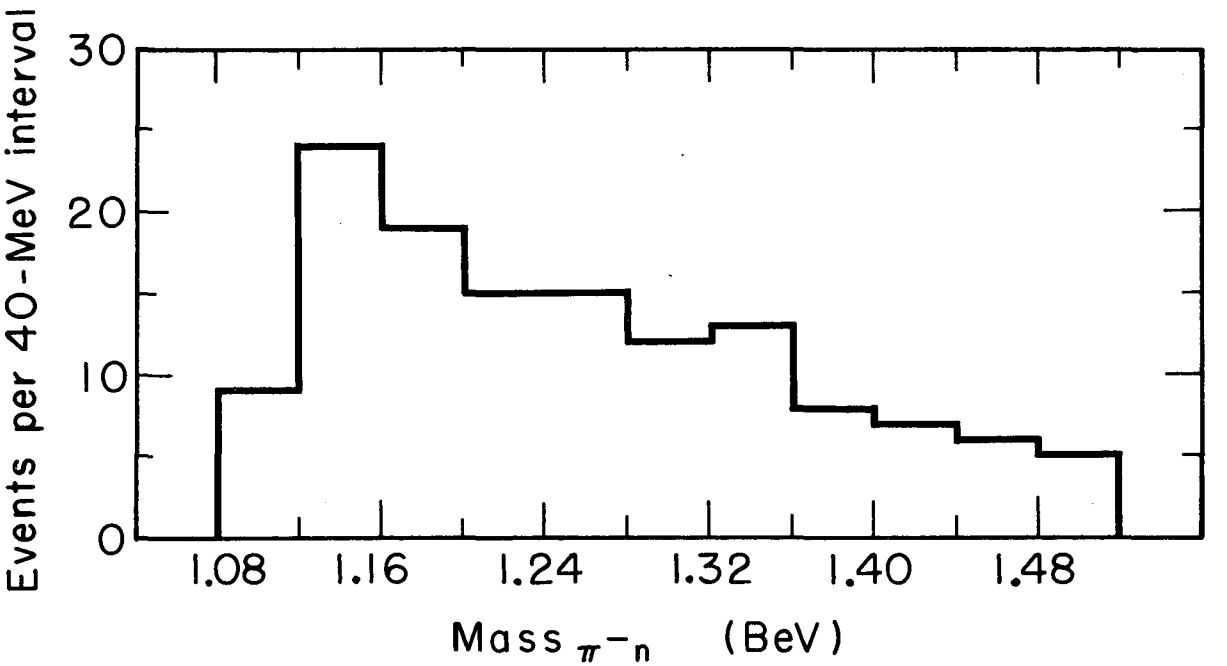

MUB-6252

Fig. 2

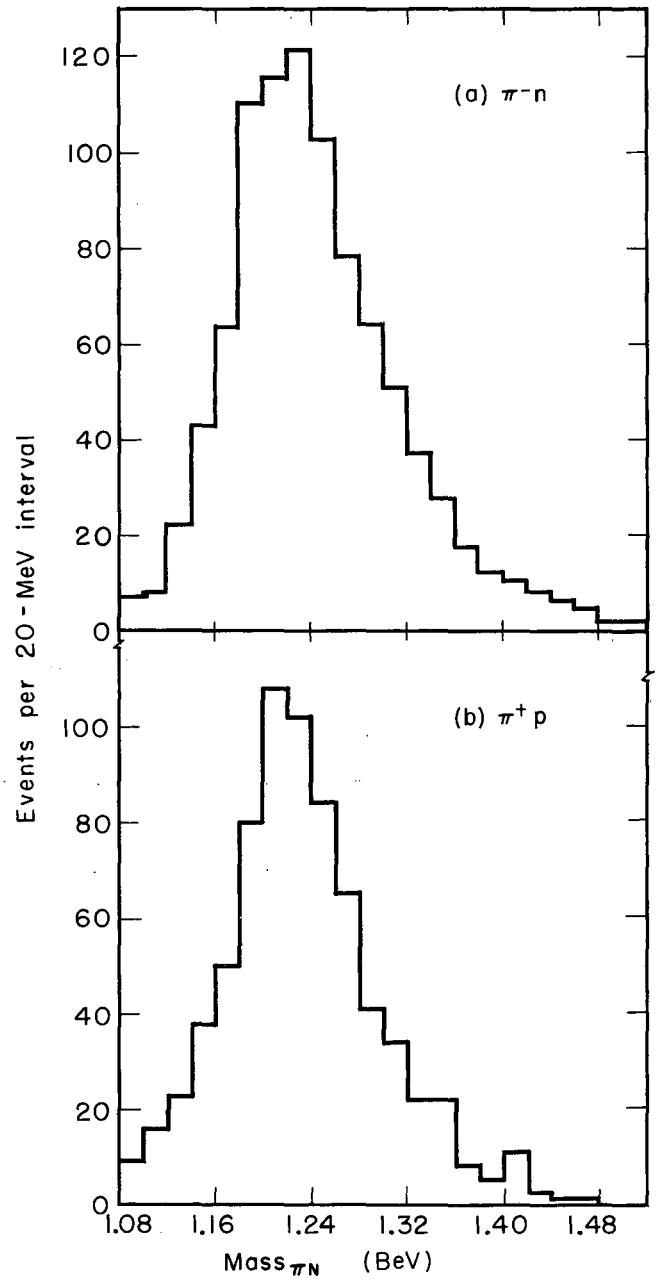
(a) $\pi^- n$
(b) $\pi^+ p$
Events per 20-MeV interval
0
20
40
60
80
100
120
1.08
1.16
1.24
1.32
1.40
1.48
Mass$_{\pi N}$ (BeV)
MUB-7413

Fig. 3

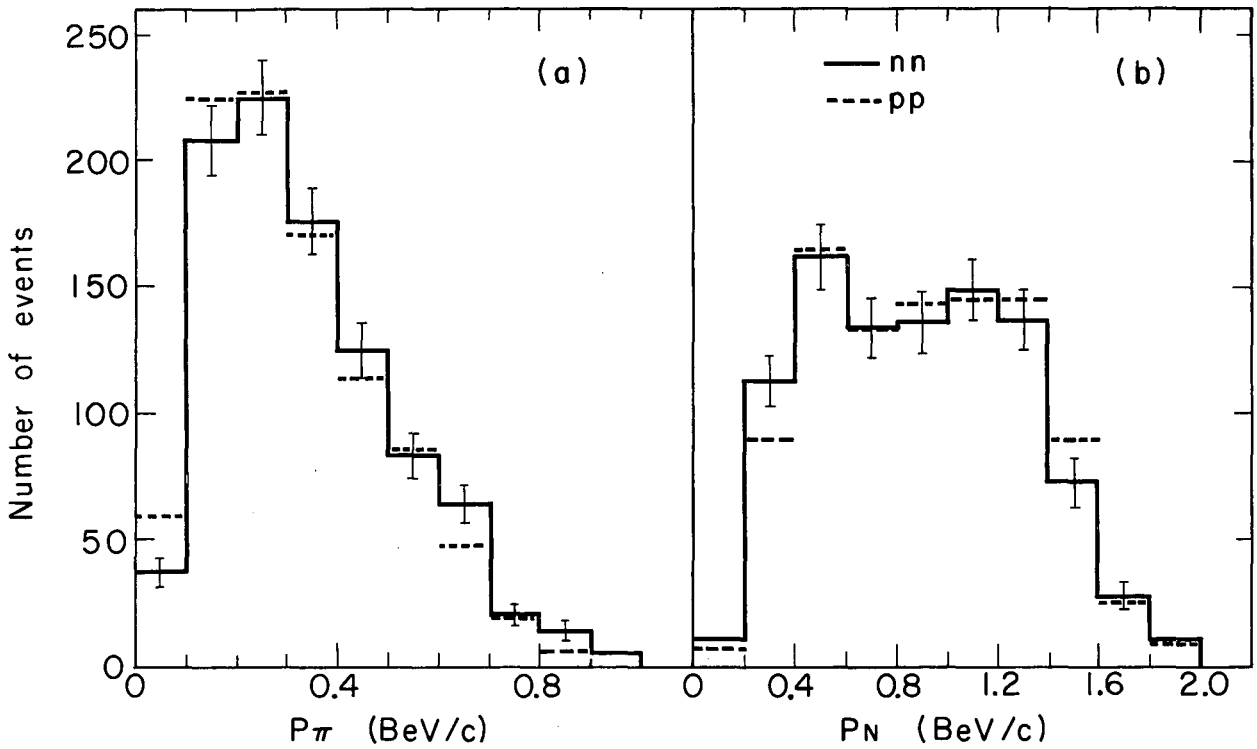

MUB-6255

Fig. 4

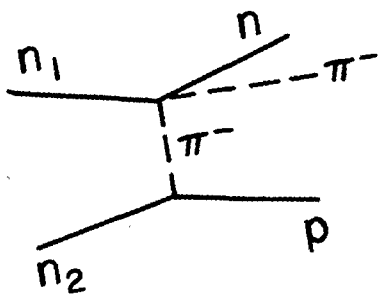

(a)

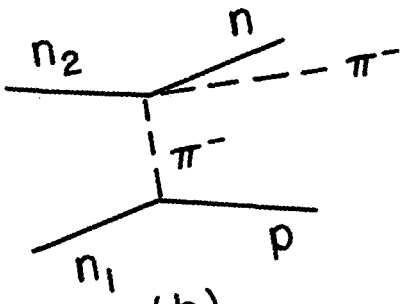

(b)

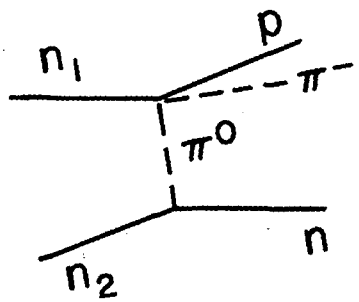

(c)

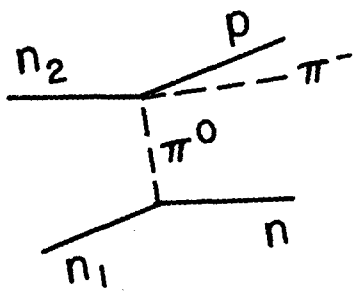

(d)

MUB-7412

Fig. 5

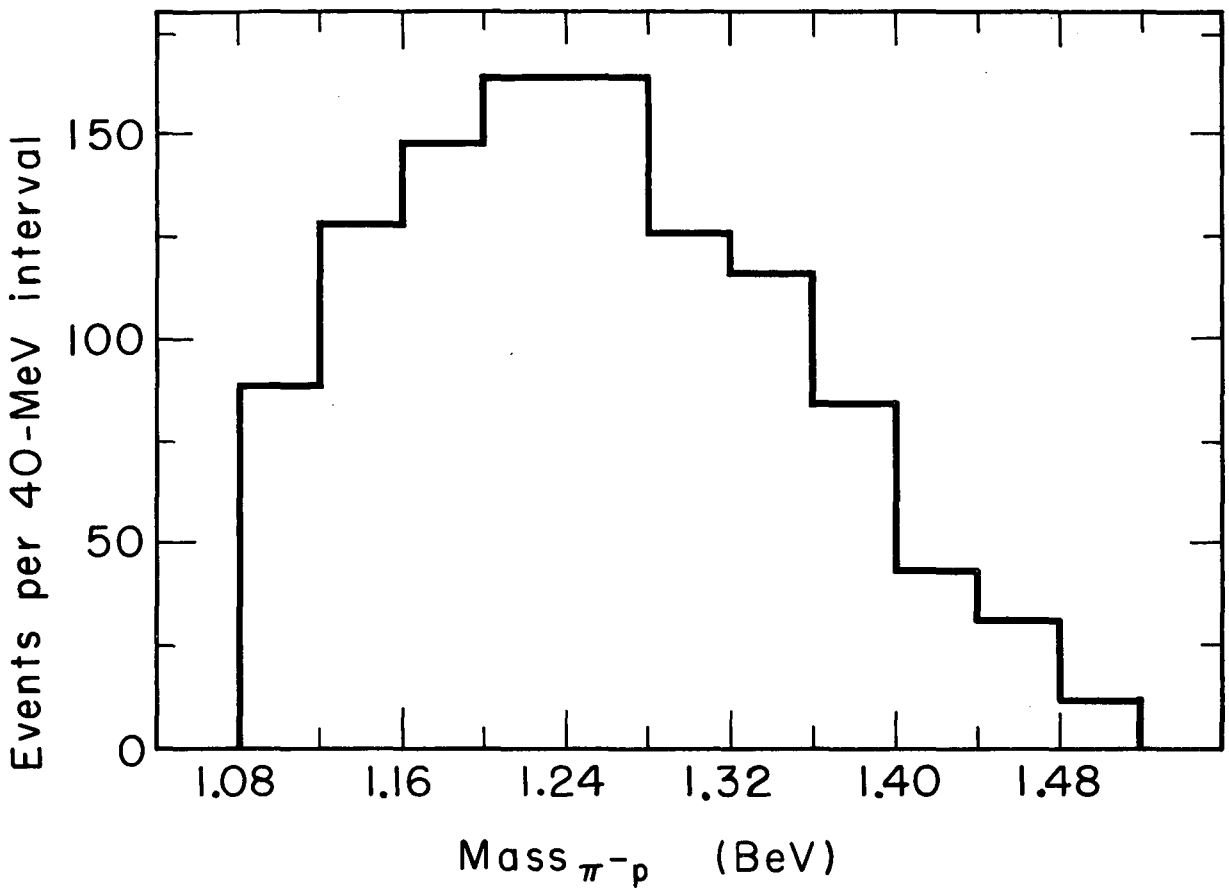

MUB-6253

Fig. 6

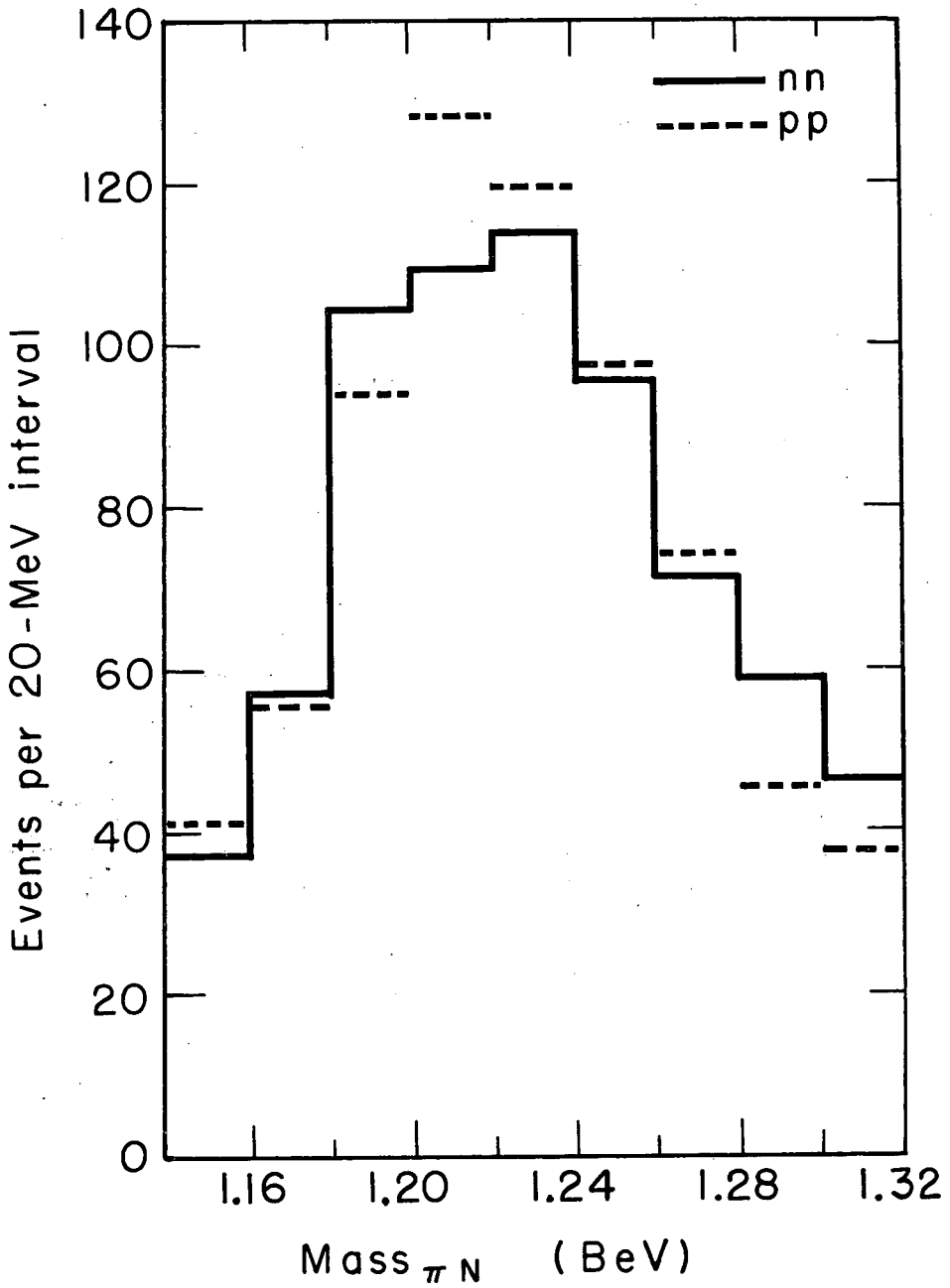

MUB-6254

Fig. 7